Shear-critical reinforced concrete beams under sustained loading Part II: Numerical study

Reza Sarkhosh, Joost Walraven, Joop den Uijl

Delft University of Technology, Faculty of Civil Engineering and Geosciences, Group of Concrete Structures, the Netherlands

In part I of this paper, dedicated to the subject of shear resistance under sustained loading (Sarkhosh 2015), a series of tests on reinforced concrete beams without shear reinforcement was described, which were subjected to high sustained shear loads close to the short-term failure load. The goal of this research project was to investigate the behaviour of shear-critical concrete beams under sustained loading. The beams were subjected to the sustained load for periods ranging from three months to three years. Meanwhile, the deflection, crack growth and crack widths were measured. In part II of this paper, a numerical model is presented based on a modification of the inclined shear crack model of Gastebled & May (2001), in which the effect of time-dependent parameters on the shear resistance of the concrete beams is introduced. The model considers a bilinear inclined shear crack in the beam web that includes the effect of aggregate interlock according to the rough crack model of Walraven (1980) on the shear resistance of the beam. The validity of the modified model was verified for short term loading against 393 experiments on concrete beams. For long term loading it was verified against new tests (Part I of this paper). With this model it can be explained why the sustained loading effect in shear is much less significant than in tension and compression.

1 Introduction

Three different mechanisms of fractural damage are involved in the shear failure of RC members without web reinforcement: a) formation of a diagonal shear crack, mostly originating from a flexural crack b) anchorage or bond failure and c) crushing of concrete in the compression zone (Fig. 1). With respect to the location of the diagonal crack in the web, for the chronological order of these mechanisms in the failure process two possibilities exist:

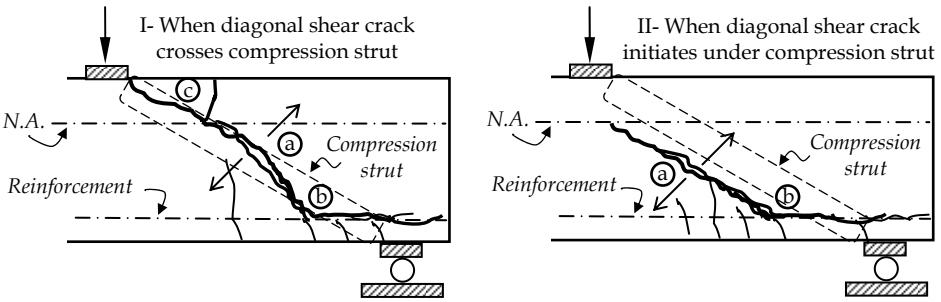

Figure 1. Mechanisms of shear fracture; (a) diagonal tension crack, (b) anchorage or bond failure and (c) crushing of concrete in the compression zone

I. A diagonal shear crack develops crossing the possible compression strut between loading plate and support (Fig. 1, left)

The first mechanism is always diagonal tension cracking which may be initiated in the web when the inclined tensile stress reaches the tensile strength of the concrete. Subsequently, the inclined crack extends in both directions or by growth of a flexural crack from the bottom of the beam, while propagating close to a 45 degree angle towards the top. In both cases, when the shear crack reaches the neutral axis, it cannot propagate any further towards the top. At that point, with sufficient stress, fracture occurs along the reinforcement at the bottom of the beam towards the anchorage, which may split the beam into two pieces. Furthermore, in the absence of compression reinforcement, the concrete in the compression zone fails at the top by breaking out of the triangular zone c.

II. A diagonal shear crack is initiated and propagates below the possible compression strut between loading plate and support (Fig. 1, right)

The diagonal shear crack is initiated by a flexural crack from the bottom, while propagating under the compression strut towards the top. In this case, the shear crack grows to the neutral axis under the loading plate and cannot propagate any further towards the top. At that point, the fracture process zone in front of the crack tip is confined by compressive stresses in both x and y directions due to flexure and the effect of the loading plate. Thus, crushing of the beam as a consequence of the shear crack requires extra stresses. In this case, a higher shear resistance of the beam may be found.

As a conclusion, the behaviour of the shear-flexure crack as the most important mechanism of failure in slender beams with an a/d ratio (shear slenderness ratio, see also Fig. 2)

between 2.5 and 6.0, should be well studied in order to be able to explain and simulate the time dependent performance of a shear critical beam.

2 Research significance

In this paper, two models, one based on a shear crack with a linear shape and the other based on a shear crack with a bilinear shape will be compared with regard to their ability to predict the shear resistance both for monotonic short term loading and for sustained loading. The linear shape of the shear crack corresponds with the model of Gastebled & May (2001) and the bilinear shape of the shear crack is a modification of this model, which allows to consider aggregate interlock as a component of the shear resistance of the beam. The analytical model of Gastebled & May assumes that the shear resistance is reached when the inclined crack starts to propagate, and sufficient energy is released at the level of the longitudinal reinforcement. However, this model does not consider the effect of aggregate interlock and therefore underestimates the shear resistance of the beam. The analytical model proposed in this chapter, which will later be verified with experiments, predicts a more accurate shear resistance of reinforced concrete members without stirrups by virtue of the use of the aggregate interlock effect. Furthermore, an evaluation is presented in which the effect of various parameters under sustained loading is discussed.

3 Shear resistance according to Gastebled & May, and Xu et al.

By the time that the crack tip reaches the neutral axis, the fracture mechanism is associated with opening of the crack by a rotation around the crack tip. Moreover the formulation of the model is based on the fundamental relation of linear elastic fracture mechanics, being $U_e = \frac{1}{2}\delta W_{ext}$, where U_e is the potential elastic energy and δW_{ext} is the external work done by the applied force. The mechanism producing external work is rotation, under a constant load, around the tip of the diagonal crack. In order to calculate the energy release, the rotational stiffness of the beam needs to be determined. To that aim, the bulk of uncracked concrete and the embedded reinforcement are considered to behave as a rigid body except for the concrete connection subjected to compression. The rotational stiffness depends on the axial and the dowel stiffness of the longitudinal reinforcement, itself depending on the extent of splitting releasing the reinforcing bar (Reineck, 1991; Gastebled & May, 2001 and Xu et al., 2012). The stiffness is worked out considering the free body diagram of a diagonal shear crack, see Fig. 2.

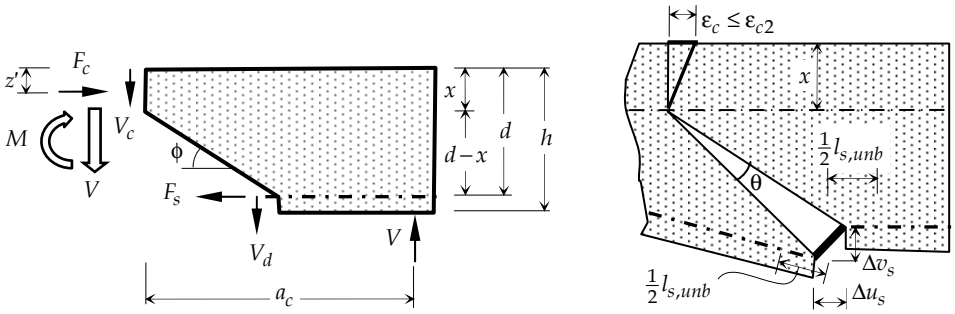

Figure 2. Free body diagram of a diagonal shear crack with a linear pattern in reinforced concrete

The axial and shear (dowel) force in the steel bar crossing the diagonal crack can be linked to the crack opening (rotational) angle θ using the elastic properties of the bar and the geometry of the deformation mechanism. When the shear crack reaches the neutral axis, the following equations apply:

$$F_s = \frac{E_s A_s}{l_{s,unb}} \Delta u_s = \frac{E_s A_s}{l_{s,unb}} (d - x)\theta \tag{1}$$

$$V_d = \frac{G_s \Sigma_s}{l_{s,unb}} \Delta v_s = \frac{9}{26} \frac{E_s A_s}{l_{s,unb}} \frac{(d - x)\theta}{\tan\phi} \tag{2}$$

where E_s and G_s are the modulus of elasticity and the shear modulus of the reinforcing steel, Σ_s is the reduced cross-section of the bar according to Gastebled & May, and $l_{s,unb}$ is the unbonded length of the reinforcement. G_s and Σ_s can be expressed as:

$$G_s = \frac{E_s}{2(1 + \nu_s)} = \frac{E_s}{2.6} \tag{3}$$

$$\Sigma_s = 0.9 A_s \tag{4}$$

The crack width in the longitudinal direction can be written as:

$$\Delta u_s = s_{cr} (\varepsilon_s - \frac{\sigma_{ts}}{E_c}) \tag{5}$$

where ε_s is the strain in the steel, σ_{ts} is the mean stress in the concrete regarding tension stiffening, and s_{cr} is the crack spacing, which is equal to:

$$s_{cr} = \alpha_c \, s_c \tag{6}$$

where s_c is the maximum crack spacing, and $0.5 \leq \alpha_c \leq 1.0$ according to Marti et al. (1998) or $\alpha_c = 0.71$ according to Reineck (1991).

Tension stiffening (Clark & Spiers, 1978; Gilbert & Warner, 1978; Hsu & Zhang, 1996; Wu & Gilbert, 2008; Wu, 2010 and Lárusson et al., 2012) represents the tensile stress transfer resistance of concrete via the bond between concrete and reinforcement. This is reflected by the fact that a cracked reinforced concrete member in tension is stiffer than the naked bar.

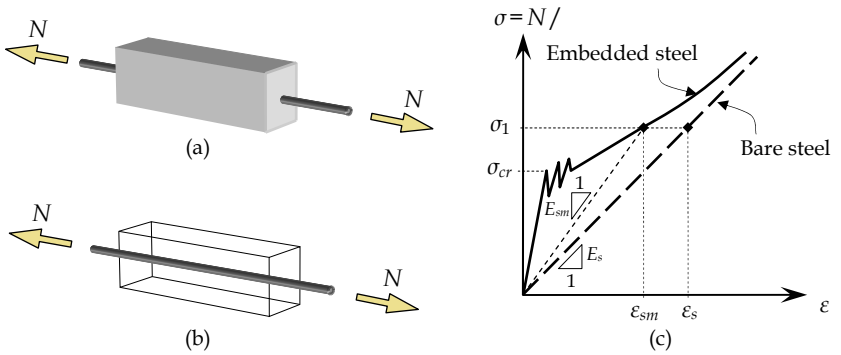

Figure 3. Concrete tension stiffening: (a) tension chord with embedded reinforcing steel; (b) bare reinforcing bar; (c) comparison of stiffness of embedded steel and bare steel bar according to Wu, (2010) and Lárusson et al. (2012)

With respect to the free body diagram shown in Fig. 2, a set of equilibrium equations can be formulated:

$$F_s = F_c \tag{7}$$

$$V = V_d + V_c \tag{8}$$

$$V\,a_c = V_d \frac{d-x}{\tan\phi} + F_s(d-z') \tag{9}$$

Substitution of F_s and V_d from Eqs. 1 and 2 into Eq. 9, results in:

$$V = \frac{E_s A_s (d-x)}{a_c}\left[\frac{9}{26}\frac{d-x}{\tan^2\phi} + d - z'\right]\frac{\theta}{l_{s,unb}} \tag{10}$$

According to the fundamental relation of fracture mechanics and the energy theorem, at the critical fracture state, when the required energy for fracture is released, the variation of

the extra force work can be expressed as two times the variation of the energy required for critical crack propagation:

$$M\ \delta\theta = \delta W = 2\ \delta l_{s,unb}\ b\ G_f \tag{11}$$

where G_f is the fracture energy required for crack propagation in any cracked solid body with a given width of b. Accordingly, the shear resistance of the beam is calculated as given by Gastebled & May:

$$V_u = \frac{\sqrt{2G_f b E_s A_s (d-x)\left[\frac{9}{26}\frac{d-x}{\tan^2\phi} + d - z'\right]}}{a_c} \tag{12}$$

$$G_{f,MC90} = (0.0469\, d_g^2 - 0.5\, d_g + 26)(\tfrac{1}{10} f_c)^{0.7} \tag{13}$$

where d_g is the maximum aggregate size that is assumed to be 20 mm, and f_c is the concrete cylinder compressive strength. A semi-empirical formula for the calculation of the position of the diagonal crack was proposed by Kim and White (1991):

$$a_c = 3.3\, a_s \left[\frac{\rho (d/a_s)^2}{(1-\sqrt{\rho})^2}\right]^{\frac{1}{3}} \tag{14}$$

where ρ is the reinforcement ration of the concrete member. In the research of Gastebled & May, the depth of the compression zone x is assumed to be $x = 0.2\ d$ and $z' = 0.1$ d . Also, the angle of the shear crack ϕ is assumed to be 45° and the fracture energy is taken from the MC90's expression (eq. 13). Xu, Zhang and Reinhardt (2012) developed this model using the mode-II fracture energy, which is calculated as $G_{IIf} = K_{IIc2} / E_c$ (Sarkhosh, 2014).

4 Behaviour of a shear crack under sustained loading

After the shear crack has reached the neutral axis, under the effect of sustained loading two mechanisms are expected to occur: the first mechanism is crack opening at the middle of the crack, due to a reduction of the modulus of elasticity in time (effect of creep). Initially, the bond creep is assumed to be zero and therefore the tensile force and the dowel force of the reinforcement remain the same. Subsequently, the effect of bond creep is introduced leading to opening of the crack at the level of the reinforcement.
If the bond creep is assumed to be 0, the following expression can be derived:

$$F_s(t) = F_{s0} = \frac{E_s A_s}{l_{s,unb}} \Delta u_s = \frac{E_s A_s}{l_{s,unb}} (d - x)\theta_0 \tag{15}$$

$$V_d(t) = V_{d0} = \frac{G_s \Sigma_s}{l_{s,unb}} \Delta v_s = \frac{9}{26} \frac{E_s A_s}{l_{s,unb}} \frac{(d - x)\theta_0}{\tan\phi} \tag{16}$$

where θ_0 is the shear crack opening angle (Fig. 2, right) due to immediate loading by V at time t_0 .

$$V = \lambda V_u = \frac{E_s A_s (d - x)}{a_c} \left[\frac{9}{26} \frac{d - x}{\tan^2 \phi} + d - z' \right] \frac{\theta_0}{l_{s,unb}} \tag{17}$$

where λ is the load intensity factor (ratio of sustained load to ultimate load). Here, if the external work done by the applied force δW is less than two times the elastic potential energy for fracturing U_e , fracture does not occur, so:

$$\frac{1}{2} \delta W \le U_e \tag{18}$$

$$\frac{1}{2} \delta W = \frac{1}{2} M \delta\theta = \frac{1}{2} (M \delta\theta_0 + M \delta\theta_{creep}) = \lambda V_u a_c \frac{1}{2} \delta(\theta_0 + \theta_{creep}) \tag{19}$$

$$U_e = G_f(t) b \, \delta l_{s,unb} \tag{20}$$

where θ_{creep} is the crack opening angle due to the creep effect, which can be written as a function of the initial crack opening angle θ_0 :

$$\theta_{creep} = \theta_0 \varphi_w \tag{21}$$

where φ_w is a function of the opening of the crack due to the effect of creep. Accordingly:

$$\lambda V_u < \frac{1}{a_c} \sqrt{2 G_f(t) b E_s A_s \frac{d - x}{1 + \varphi_w} \left[\frac{9}{26} \frac{d - x}{\tan^2 \phi} + d - z' \right]} = V_u(t) \tag{22}$$

where V_u follows from Eq. 12 and λ is the load intensity factor. Now, the margin of shear safety can be introduced as:

$$\varsigma = \frac{V_u(t)}{\lambda V_u} = \frac{1}{\lambda} \sqrt{\frac{G_f(t) / G_f(t_0)}{1 + \varphi_w}} > 1 \tag{23}$$

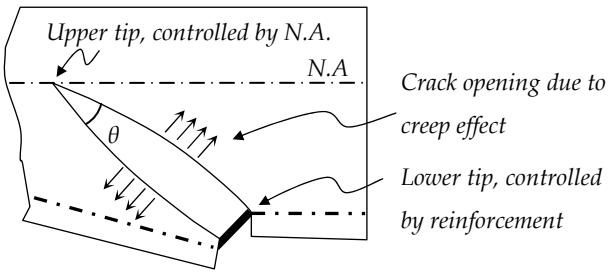

Figure 4. A crack that opens at mid-height due to the creep effect

Effect of bond creep

In a concrete beam, shear-flexure cracks as well as shear-tension cracks result from a tensile stress in the concrete caused by external (e.g. applied load) effects. When the crack reaches the reinforcing bars, the opening of the crack is controlled by the quality of bond between concrete and steel. Under sustained loading, the neighbourhood of a crack is affected by creep of the concrete adjacent to the reinforcing steel, which results in an increase of the slip between concrete and steel in time.

In time dependent problems, two counteracting mechanisms play the most significant roles in widening of the crack near the reinforcement. The concrete tensile stress associated with tension stiffening induced creep deformation contributes to an expansion of the concrete between the cracks, which obviously reduces the crack opening. On the other hand, drying shrinkage causes a volume reduction in the concrete blocks between the cracks, which results into a gradual opening of the cracks (Chong, 2004). The crack widening in time at the level of the reinforcement is:

$$\Delta u_s(t) = s_{cr}\left[\varepsilon_s(t) - \left(\frac{\sigma_{ts}(t)}{E_c} + \varepsilon_{cr}(t) + \varepsilon_{sh}(t)\right)\right] \tag{24}$$

Due to the fact that the influence of shrinkage on widening of the crack is far more dominant than the influence of concrete tensile stress and creep in closing the crack, the width of a crack in a RC concrete member generally increases with time. The crack widening according to Eq. 24 can be written in form of a creep function as:

$$\Delta u_s(t) = \Delta u_{s0}(1 + \varphi_{bond}) \tag{25}$$

where Δu_{s0} is the crack widening at time t_0 and φ_{bond} is the bond creep coefficient.

Here again, the crack opening angle increases in time due to bond creep and if the external work due to sustained loading is smaller than the required energy for fracture, the beam does not fail:

$$\alpha_c \, \delta\theta \, \lambda \, V_u < \frac{2 G_f(t) \, b \, \delta l_{s,unb}}{(1+\varphi_{bond})(1+\varphi_w)} \tag{26}$$

Therefore, the shear safety margin ς under sustained loading can be written as:

$$\varsigma = \frac{v_u(t)}{\lambda v_u(t_0)} = \frac{1}{\lambda} \sqrt{\frac{G_f(t)/G_f(t_0)}{(1+\varphi_{bond})(1+\varphi_0)}} > 1 \tag{27}$$

Eq. 27 is suitable for the sake of analysis where the creep of bond and the creep of concrete can be well estimated. However, in experiments, it is perhaps difficult to separate the crack opening due to creep of concrete and due to bond creep. Therefore a ratio of crack width at time t to the width at time t0 can be formulated as:

$$\varsigma = \frac{1}{\lambda} \sqrt{\frac{G_f(t)/G_f(t_0)}{w(t)/w(t_0)}} > 1 \tag{28}$$

where $w(t)$ and $w(t_0)$ are crack widths at times t and t_0 , respectively.

If the normal and shear stresses across the crack surface are known, the crack width can be calculated according to Frénay (1989, 1990 and 1991). Based on experiments on time-dependent shear transfer on plain and reinforced concrete specimens with a single crack, Frénay proposed an empirical model for the development of crack width and crack sliding in time:

$$w(t) = w(t_0)[1+\varphi_w(t)] \tag{29}$$

$$\delta(t) = \delta(t_0)[1+\varphi_s(t)] \tag{30}$$

where φ_w and φ_s are creep coefficients for the crack width w and the crack sliding δ, respectively. The creep coefficients are given for a cube concrete strength between 30 MPa and 70 Mpa, reinforcement ratio ρ_s = 0, 1.12% and 2.24%, and for different normal and shear stresses on the crack.

5 Shear failure model based on bilinear shear crack

The model with the linear inclined shear crack, presented in the previous section, does not consider the effect of aggregate interlock, which has been proven to play an important role in the shear strength of concrete beams (Yang, 2014). To overcome that disadvantage, a nonlinear crack pattern is assumed as presented in Fig. 5. Here, the sliding of the crack in the lower part can be related to the angle of rotation θ, and the horizontal length of the crack a_{cc} .

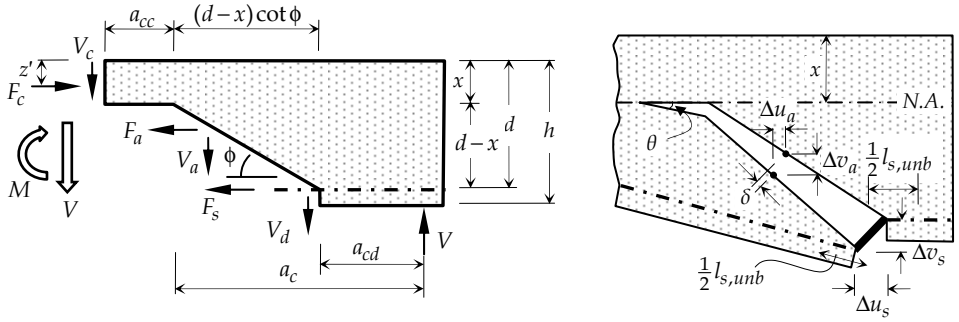

Figure 5. Free body diagram of a bilinear shear crack in reinforced concrete

By means of the elastic properties of the bar and the geometry of the deformation mechanism, the axial and shear (dowel) force in the steel bar crossing the diagonal crack can be associated with the angle of rotation θ and the length of the horizontal part of the crack a_{cc} . When the shear crack reaches the neutral axis, the following equations can be formulated:

$$F_s = \frac{E_s A_s}{l_{s,unb}} \Delta u_s = \frac{E_s A_s}{l_{s,unb}} (d-x)\theta \tag{31}$$

$$V_d = \frac{G_s \Sigma_s}{l_{s,unb}} \Delta v_s = \frac{9}{26} \frac{E_s A_s}{l_{s,unb}} \left(\frac{d-x}{\tan\phi} + a_{cc} \right) \theta \tag{32}$$

$$F_a = \tau_a b (d-x)\cot\phi + \sigma_a b (d-x) \tag{33}$$

$$V_a = \frac{F_a \Delta v_s}{\Delta u_s} = \left(\frac{1}{\tan\phi} + \frac{a_{cc}}{d-x} \right) F_a \tag{34}$$

where F_a and V_a are the horizontal and the vertical components of the aggregate interlocking force due to shear sliding δ, respectively, b is the beam width, τ_a is the shear

stress acting across the crack faces, and σ_a is the normal stress transmitted across the crack. τ_a and σ_a can be calculated according to the rough crack model proposed by Walraven (1980). The model was later introduced in the fib Model Code 2010:

$$\tau = C_f \left\{ -0.04 f_c + \left[1.8 w^{-0.8} + \left(0.292 w^{-0.7} - 0.25 \right) f_c \right] \delta \right\} \tag{35}$$

$$\sigma = C_f \left\{ -0.06 f_c + \left[1.35 w^{-0.63} + \left(0.242 w^{-0.55} - 0.19 \right) f_c \right] \delta \right\} \tag{36}$$

where τ is the shear stress in MPa, σ is the normal stress, δ is the shear displacement (sliding), w is the crack width both in mm, and C_f is an aggregate effectivity factor, which is 1.0 if the aggregate does not fracture upon cracking of the concrete. For concrete with weak aggregates, or high strength concrete (with strong cement paste), in which most of the particles fracture at crack propagation, a value of about 0.35 applies for C_f.

In this study a simplified model for aggregate interlock is used with a linear relation for crack sliding and crack opening. Therefore, the aggregate interlock model of Eqs. (35) and (36) is approximated by:

$$\tau_a = C_f [0.125 w^{-1} f_c] \delta \tag{37}$$

$$\sigma_a = C_f [0.08 w^{-1} f_c] \delta \tag{38}$$

where w is the opening of the shear tension crack, and δ is the shear crack sliding.

The approximation of stresses due to aggregate interlock is shown in Fig. 6. For a concrete strength of f_c = 30 MPa. Eqs. (37) and (38) overestimate the stresses for small values of δ, and underestimate the stresses for large values of δ. However, the proposed model assumes that in the critical fracture state, the shear resistance can be calculated by means of the energy release due to opening of the inclined crack and debonding of reinforcement and concrete. It will be discussed later that the required energy up to fracture of the inclined crack, is related to the ratio of crack sliding to crack width δ/w. Therefore it is important that the 'approximate' values according to Eqs. (37) and (38) predict δ/w ratios for different stresses, close enough to the model of Walraven. Fig. 7 shows the δ/w ratios for shear stresses τ between 1.0 MPa and 8.0 MPa. The approximated δ – w relations show consistent results with the rough crack model of Walraven (1980).

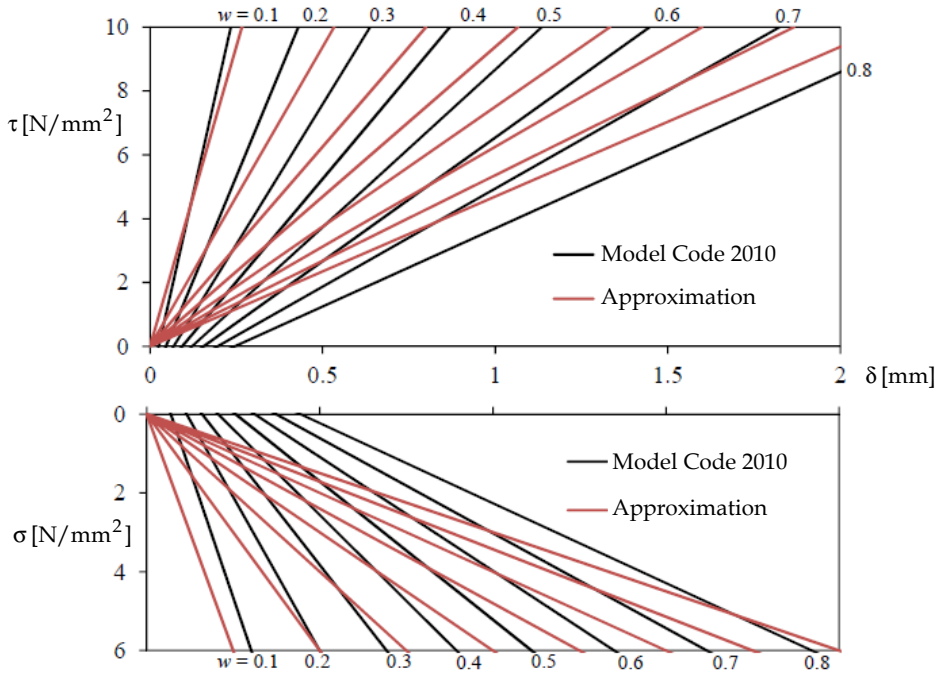

Figure 6. Relations between shear stress τ and normal stress σ, crack width w and crack sliding δ, (f_c = 30 MPa)

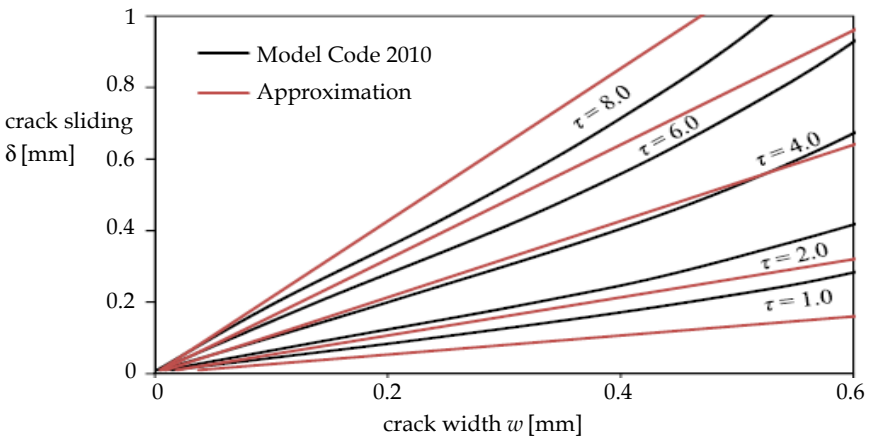

Figure 7. Relations between δ and w for different shear stresses τ (f_c = 30 MPa)

The shear crack sliding in the diagonal part of the shear crack can be formulated as (Fig. 5):

$$\delta = \Delta v_a \sin\phi - \Delta u_a \cos\phi \tag{39}$$

In the case of a linear shape of the crack (Fig. 2), the shear sliding δ is zero:

$$\delta = \frac{d-x}{\tan\phi}\theta \sin\phi - (d-x)\theta\cos\phi = 0 \tag{40}$$

whereas in the case of a bilinear crack δ follows from:

$$\delta = \left(\frac{d-x}{\tan\phi} + a_{cc}\right)\theta\sin\phi - (d-x)\theta\cos\phi = a_{cc}\,\theta\sin\phi \tag{41}$$

Substituting Eqs. (37), (38) and (41) into Eq. (33), the horizontal component of the aggregate interlock force can be written as:

$$F_a = C_f b(d-x)\left[w^{-1} f_c\, a_{cc}\,\theta\sin\phi\,(0.08 + 0.125\cot\phi)\right] \tag{42}$$

With respect to the free body diagram shown in Fig. 5, the following set of equilibrium equations is obtained:

$$F_s + F_a = F_c \tag{43}$$

$$V = V_d + V_c + V_a \tag{44}$$

$$V(a_c + a_{cc}) = V_d\left(\frac{d-x}{\tan\phi} + a_{cc}\right) + F_s(d-z') + V_a\left(\frac{d-x}{2\tan\phi} + a_{cc}\right) + F_a\left(\frac{d+x}{2} - z'\right) \tag{45}$$

Substituting F_s , V_d and F_a from Eqs. (31)-(35) into Eq. (45), yields:

$$\begin{aligned} V = {} & \frac{E_s A_s}{a_c + a_{cc}}\left[\frac{9}{26}\left(\frac{d-x}{\tan\phi} + a_{cc}\right)^2 + (d-x)(d-z')\right]\frac{\theta}{l_{s,unb}} + \\ & + \frac{C_f f_c a_{cc}\sin\phi\, b(d-x)}{a_c + a_{cc}}(0.08 + 0.125\cot\phi)\left[\frac{d-x}{2\tan^2\phi} + \frac{3a_{cc}}{2\tan\phi} + \frac{a_{cc}^2}{d-x} + \frac{d+x}{2} - z'\right]\frac{\theta}{w} \end{aligned} \tag{46}$$

According to the fundamental relation of fracture mechanics and the energy theorem, at the critical fracture state, when the required energy for fracture is released, the variation of the extra force work can be expressed as two times the variation of the energy required for critical crack propagation. As the energy is released in two regions (crushing of aggregates and debonding of concrete and steel), for each region the following equilibrium equations can be written:

$$\delta W_1 = U_{e,1} = 2\,\delta l_{s,unb}\, b\, G_{If} \tag{47}$$

$$\delta W_1 = U_{e,2} = 2\,\delta w\, b\, G_{IIf} \tag{48}$$

$$\delta W_1 = V(a_c + a_{cc})\,\delta\theta \tag{49}$$

where G_{If} and G_{IIf} are the energy consumptions in Modes I and II, respectively.

Considering $K_{IIc} = G_{IIf} E_c\, 0.5$, the shear resistance of the beam is calculated as:

$$V_u^2 = \frac{E_s A_s}{(a_c + a_{cc})^2}\left[\frac{9}{26}\left(\frac{d-x}{\tan\phi} + a_{cc}\right)^2 + (d-x)(d-z')\right] 2b G_{If} + \\ + \frac{C_f f_c a_{cc} \sin\phi\, b(d-x)}{(a_c + a_{cc})^2}(0.08 + 0.125\cot\phi)\frac{2bK_{IIc}^2}{E_c}\left[\frac{d-x}{2\tan^2\phi} + \frac{3a_{cc}}{2\tan\phi} + \frac{a_{cc}^2}{d-x} + \frac{d+x}{2} - z'\right] \tag{50}$$

in which $E_c = 22(f_{cm}/10)^{0.3}$, G_{If} is Mode I fracture energy and can be acquired from Eq. (13), and the pure Mode II fracture toughness of concrete K_{IIc} is recommended by Reinhardt & Xu (1998) to be:

$$K_{IIc} = 0.0255 f_c + 1.024 \quad [\text{MPa}\sqrt{\text{m}}] \tag{51}$$

If the depth of the compression zone x is assumed to be x = 0.2d and z' = 0.1d and the angle of the shear crack ϕ is assumed to be 45° (According to Gastebled & May), a simplified expression for the shear resistance is obtained as presented in Eq. (52). The first term is related to the shear transfer mechanism between concrete and reinforcement (bond effect) and the second term is related to the aggregate interlock effect.

$$v_u^2 = \frac{2G_{If} E_s \rho_s}{d(a_c + a_{cc})^2}\left[\frac{9}{26}(0.8d + a_{cc})^2 + 0.72d^2\right] + \\ + \frac{21.034 C_f (0.0255 f_c + 1.024)^2 f_c^{0.7} a_{cc}}{d(a_c + a_{cc})^2}\left[0.9d + \frac{3a_{cc}}{2} + \frac{a_{cc}^2}{0.8d}\right] \tag{52}$$

However, the horizontal length of the crack a_{cc} , is still unknown. For the best fit to the results, the following expression as a function of a_c , was found from a comparison with test results, as will be presented in the next section:

$$a_{cc} = 0.318\, a_c = 1.05\, a_s\left[\frac{\rho(d/a_s)^2}{(1-\sqrt{\rho})^2}\right]^{\frac{1}{3}} \tag{53}$$

6 Verification of the results of the analytical model with experiments

The shear resistance of experiments on reinforced concrete beams without stirrups, taken from the ACI-DAfStb shear database (Reineck et al., 2013), will be compared with the calculated shear resistance according to Eq. (52) as well as the recommendation of ACI 318-08 (2008), BS 8110 (1997), Eurocode 2 (2005), fib Model Code 2010 (2012) and the proposed models by Gastebled & May (2001), Bažant & Yu (2004) and Xu et al. (2012). The mean values of the empirical equations (without safety factors), which are given in Section 1.6 in Sarkhosh (2014), will be used. Moreover, a statistical analysis on the distribution of the ratio of experimental values to theoretical shear resistances ($v_{\exp} / v_{cal}$) for the various formulas is also conducted in order to further examine the quality of proposed model.

The ACI-DAfStb shear database (Reineck, 2013) includes over 1300 tests on reinforced concrete beams, which covers a wide range of the parameters of shear span to depth ratio a/d , reinforcement ratio ρ_s , effective depth d, and concrete strength f_c . The empirical equations for predicting the shear resistance of reinforced beams without stirrups are best to predict the shear-flexure failure in normal strength concrete members. Of course, the empirical equations have not been derived for the prediction of the shear resistance of beams with relatively small sizes, or very low concrete strengths. In view of that, the experiments with the following conditions have been selected from the database:

- Members with a/d ratios of at least 2.5
- Members with ρ_s ratios of at least 0.7
- Members with effective depths d higher than 150 mm
- Members with f_c higher than 20 MPa and lower than 110 MPa
- Members with b > 50 mm

Accordingly, a total number of 393 experiments from the shear database have met the criteria given above and have been selected for the further comparison of the various formulas. The summary of the experiments and the calculated shear resistances have been presented by Sarkhosh (2014). The results of the statistical evaluations using all 393 beams are given in Table 1, where the ratio of $v_{\exp}/v_{cal}$ according to Eq. (52) is reasonably close to the expected value of 1.0 with a coefficient of variation COV = 0.163. It should be noted that the value of $v_{\exp}/v_{cal}$ = 1.0 is obtained by means of the assumed value of a_{cc} in Eq. (53)

The calculated shear resistance according to *fib* MC2010 is based on the Level II approximation and gives the same results as the model given in CSA-04.

It can also be seen in Table 1 that almost all empirical formulas (except the model proposed by Bažant & Yu) give a lower mean value of the shear resistance v_{cal} than the experiments $v_{\exp}$. In the proposed model of Bažant & Yu the parameter $\kappa_0 = 0.457$ for the mean shear resistance, gives an overestimated shear resistance, but nevertheless this model and the fib MC2010 model give the lowest coefficient of variation in comparison with the other models.

Table 1. Statistical analysis for $v_{\exp}/v_{cal}$ ratio of the various calculation equations

	ACI 318-08	EC2/ MC90	MC10/ CSA04	BS 8110	Bažant & Yu	Gastebled & May	Xu et al.	Eq. 52
Mean	1.32	1.13	0.92	1.16	0.87	1.43	1.22	1.00
SD	0.284	0.171	0.124	0.172	0.115	0.218	0.211	0.163
COV	0.215	0.150	0.134	0.148	0.133	0.152	0.173	0.163
LCL5%*	0.85	0.85	0.72	0.88	0.68	1.07	0.87	0.73
UCL95%*	1.79	1.42	1.13	1.45	1.06	1.78	1.56	1.27

*Lower and upper confidence limit: $LCL_{5\%}$ = Mean –1.645 SD ; $UCL_{95\%}$ = Mean +1.645 SD

As shown in Fig. 8, the proposed model according to Eq. 52 is able to give the closest shear resistance to the experiments while the model of Gastebled & May gives the most conservative results. Fig. 9 shows the plot of the $v_{\exp}/v_{cal}$ ratio of the various calculation equations against the reinforcement ratio ρ_s. It can be seen from Fig. 9 that an increase of the reinforcement ratio, causes a slight underestimation in the prediction of the shear resistance. The best prediction of the shear resistance is related to the beams with a reinforcement ratio between 1.0 and 2.5, which is most representative for structures in practice.

The size effect on the prediction of the shear resistance of RC beams without stirrups is shown in Fig. 10. In the experiments of Bhal (1969), Kostovos (1997), Walraven (1978) and Taylor (1972), a decrease of the nominal shear resistance $v_{\exp}$ is observed as the beam depth increases. However, not all models are able to accurately predict the nominal shear resistance as the effective depth increases (Fig. 10, left). The size effect is not considered in the ACI 318-08 provision, so the shear resistance according to this model for effective

depths d lower than 300 mm is very conservative. Although the shear resistance of members with small sizes is governed by the mix design, which results in a high scatter of some models, as shown in Fig. 10, the $v_{\exp}/v_{cal}$ ratio according to Eq. (52) is very close to the expected value of 1.0.

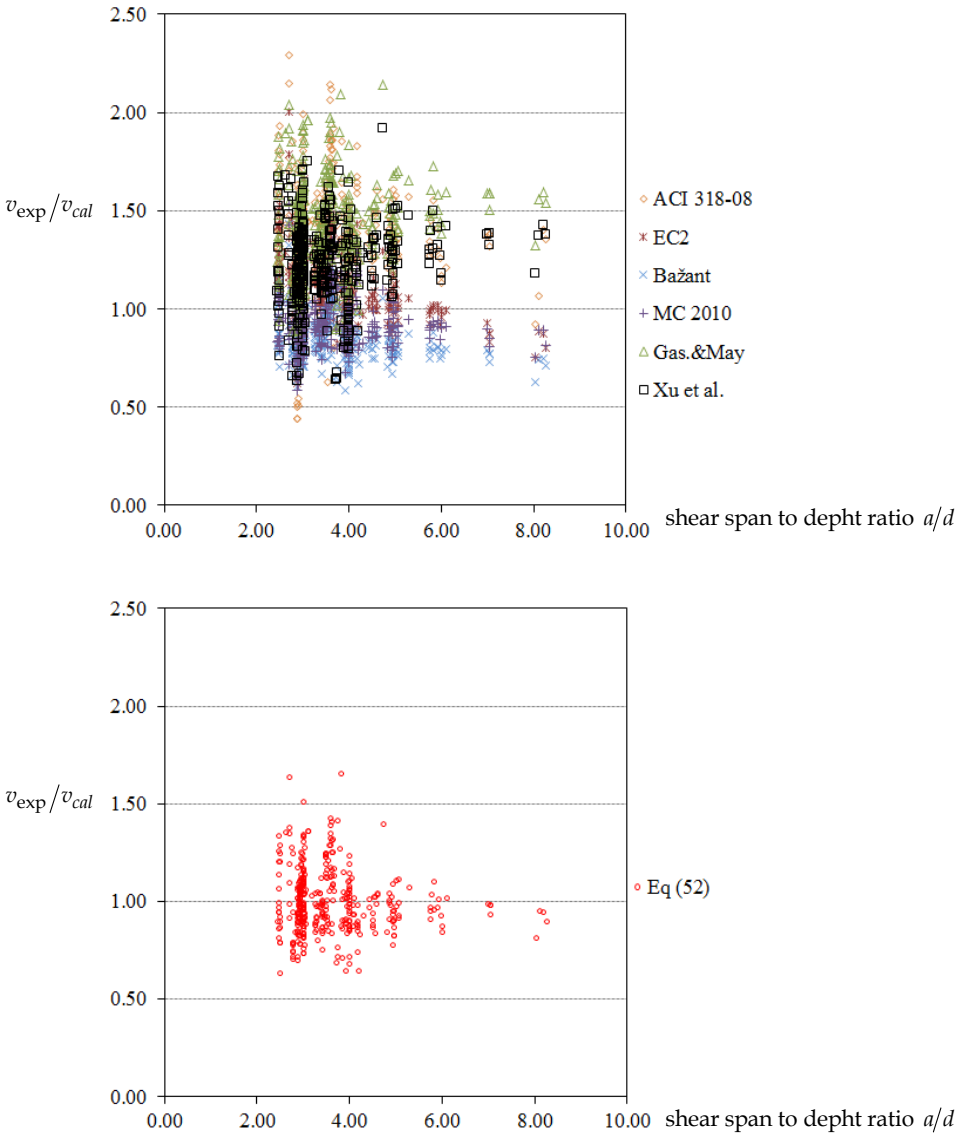

Figure 8. $v_{\exp}/v_{cal}$ as a function of a/d

Fig. 13 shows the effect of concrete strength on the prediction of the shear resistance of concrete beams by the various equations. In case of low and normal strength concrete (f_c < 70 N/mm²), the shear resistance prediction according to Gastebled & May and ACI 318-08 generally underestimates the shear resistance.

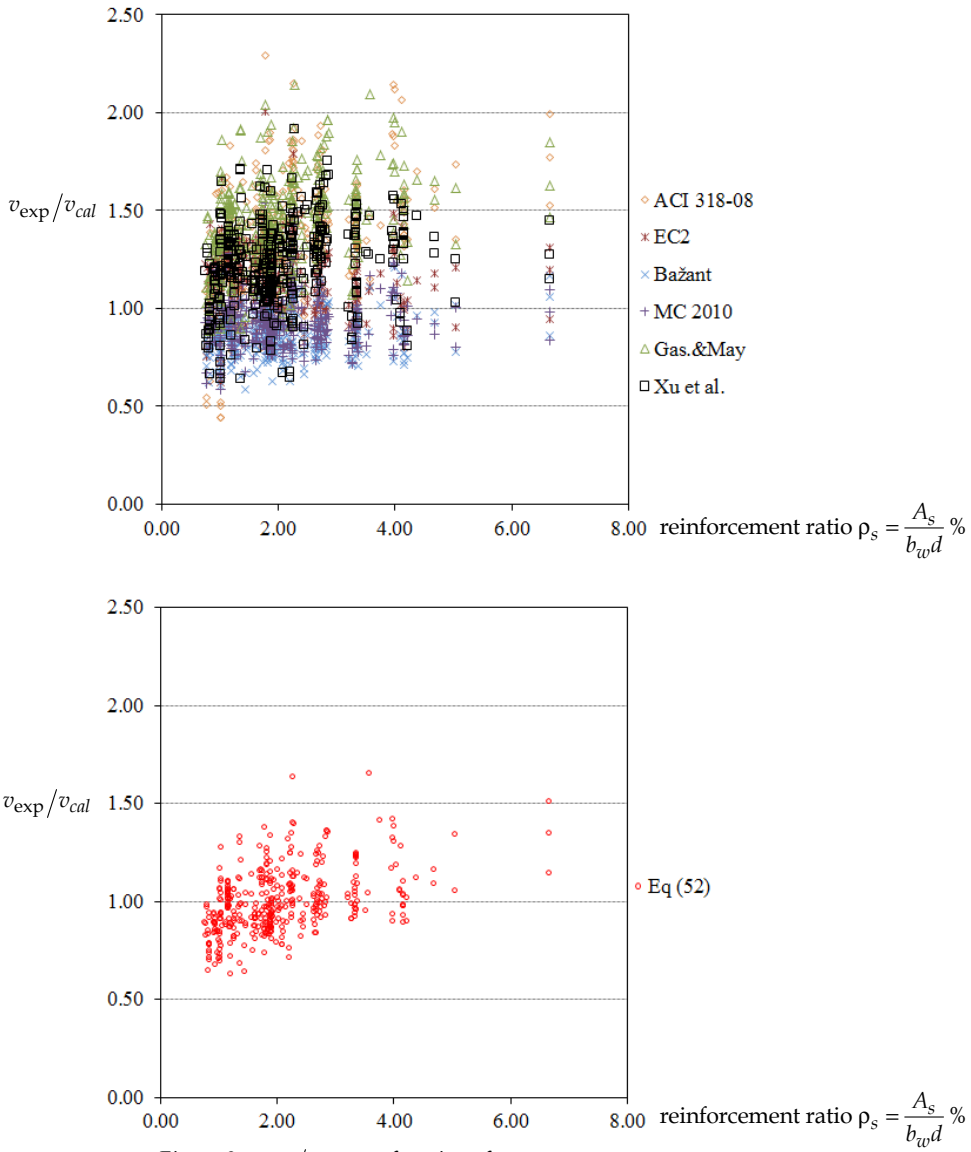

Figure 9. v_{exp}/v_{cal} *as a function of* ρ_s

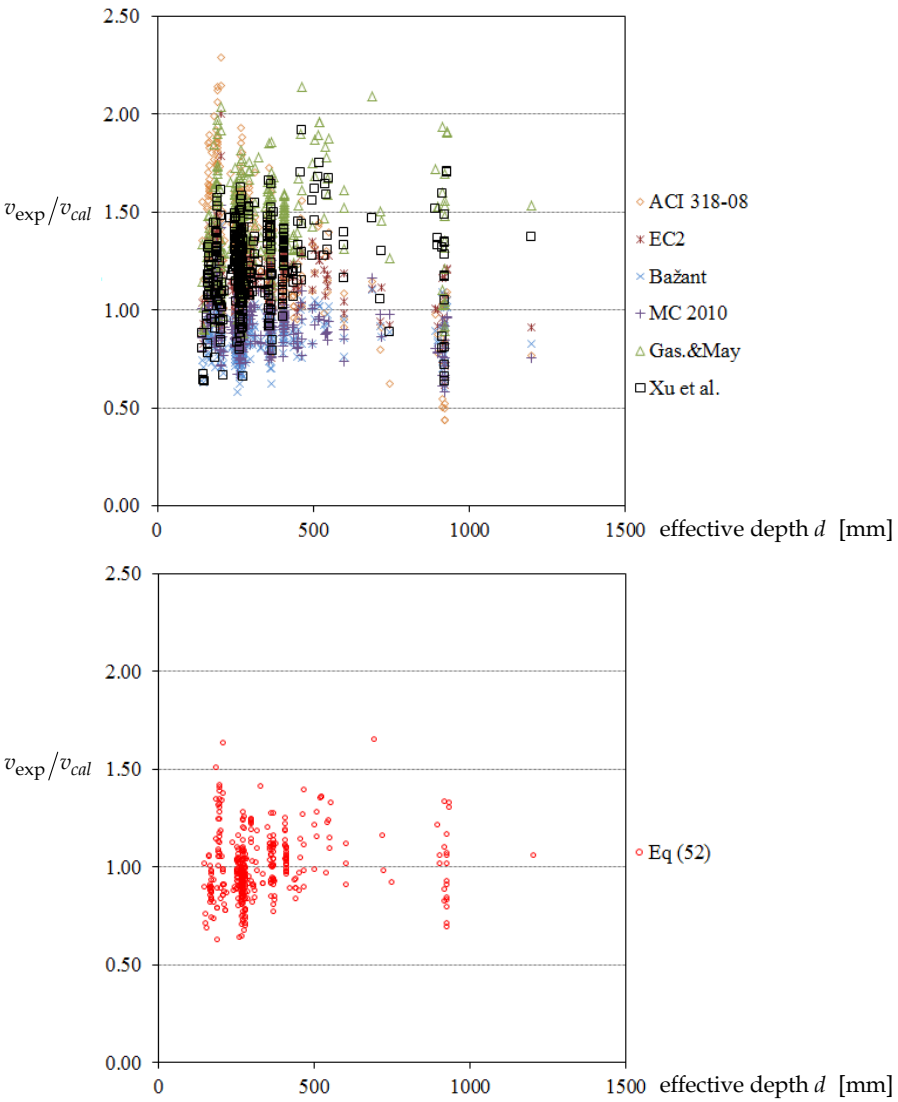

Figure 10. v_{exp}/v_{cal} *as a function of d*

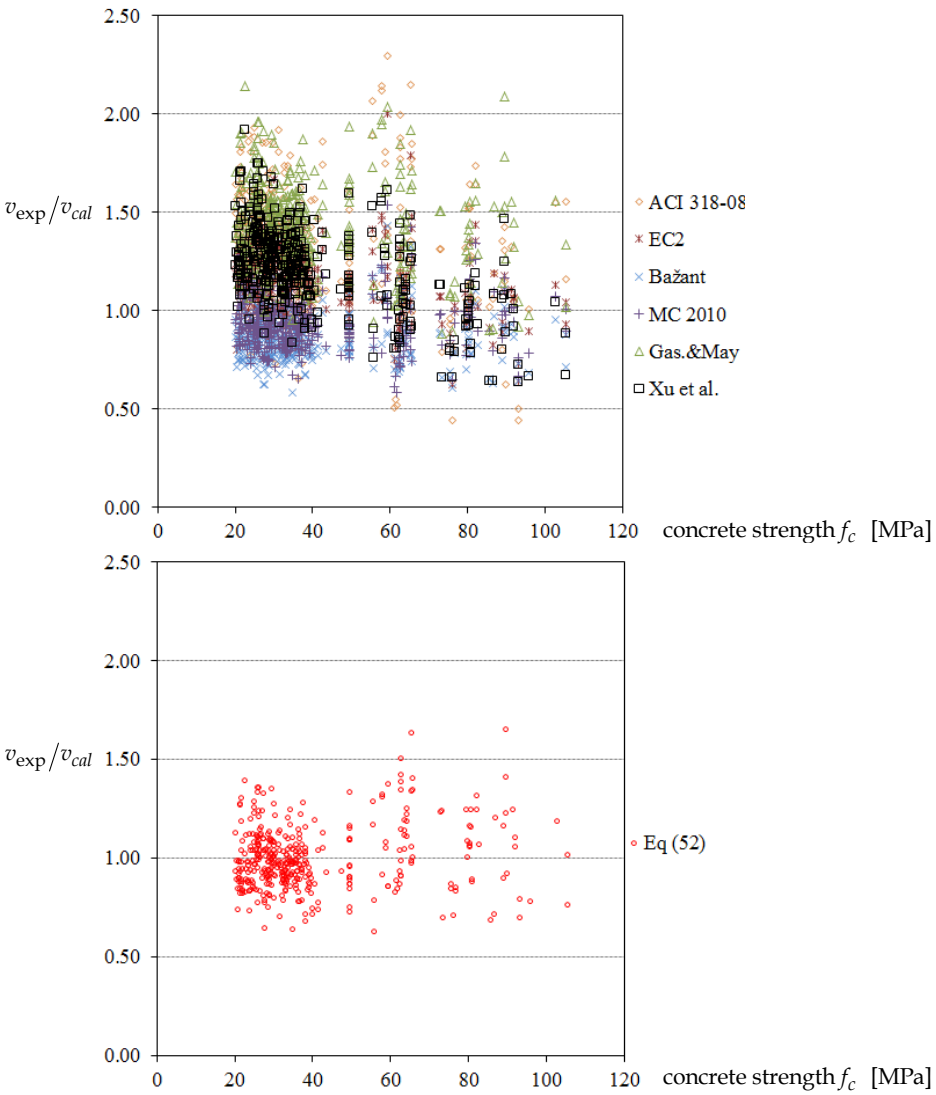

Figure 11. v_{exp}/v_{cal} *as a function of* f_c

7 Extension of the bilinear crack model to include sustained loading

Similar to the linear crack model, the bilinear crack model under sustained long-term loading involves the creep effect:

$$v_u^2(t) = \frac{2G_{If}(t)E_s\rho_s}{d[w(t)/w(t_0)](a_c + a_{cc})^2}\left[\frac{9}{26}(0.8d + a_{cc})^2 + 0.72d^2\right] + \\ + \frac{21.034C_f a_{cc}[0.0255f_c(t) + 1.024]^2[f_c(t)]^{0.7}}{d[w(t)/w(t_0)](a_c + a_{cc})^2}\left[0.9d + \frac{3a_{cc}}{2} + \frac{a_{cc}^2}{0.8d}\right] \tag{54}$$

Clearly, the time dependent shear resistance of the bilinear crack model depends on several parameters such as the reinforcement ratio ρ_c and the length of the horizontal part of the shear crack a_{cc} and is, admittedly, too complicated for practical use. However it offers the opportunity to evaluate the effect of time-dependent parameters such as $G_f(t)$, $f_c(t)$ and $w(t)$ on the shear resistance of reinforced concrete beams. Therefore, a parametric study will be carried out to investigate those effects.

In order to verify the analytical model for inclined shear cracking under sustained loading, the shear safety margin is calculated according to Eq. (55) for all 14 beams, which have been tested in long-term loading (Sarkhosh, 2014):

$$\varsigma = \frac{v_u(t)}{\lambda v_u} > 1 \tag{55}$$

where v_u and $v_u(t)$ are given in Eqs. (52) and (54), respectively, and λ is the load intensity factor, defined as the ratio between loading level in the sustained loading test and the mean shear resistance at short term loading.

The time-dependent parameters such as the ratio of concrete strength at time t to the strength at time $t_0[f_c(t)/f_c(t_0)]$, the ratio of midspan deflection at time t to the deflection at time $t_0[\Delta(t)/\Delta(t_0)]$, the mean and maximum of the crack width $[w(t)/w(t_0)]_{\text{mean}}$, $[w(t)/w(t_0)]_{\max}$ and the ratio of the diagonal deformation $DD(t)/DD(t_0)$ have been measured in time for each specimen and the results are given in Table 2. The fracture energy at time t is calculated according to Eq. (58).

$$f_{cm}(t) = \beta_{cc(}(t)\, f_{cm} \text{ (according to fib MC2010 and EC2)} \tag{56}$$

$$G_f(t) = 73[f_{cm}(t)]^{0.18} \tag{57}$$

$$G_f(t) = G_f\,[\beta_{cc}(t)]^{0.18} \tag{58}$$

where $f_{cm}(t)$ is the mean concrete compressive strength at an age of t days, $\beta_{cc}(t)$ is the time development function and s, a and β are constants, which depend on the strength class of cement and curing conditions.

In Eq. (54) the ratio of crack width $w(t)/w(t_0)$ should be calculated for the critical shear crack. However, the maximum crack width ratio $[w(t)/w(t_0)]_{\max}$ was sometimes difficult to measure for a single crack, particularly shortly after load application. This explains the lack of data in the row regarding $[w(t)/w(t_0)]_{\max}$ in Table 2. On the other hand, considering the mean value of crack width ratio $[w(t)/w(t_0)]_{\text{mean}}$ is also not appropriate due to stress redistribution in the beam which causes closing of some cracks and opening of some other cracks. If the shear safety margin ς_1 is calculated according to Eq. (59), by means of the ratio of $[w(t)/w(t_0)]_{\text{mean}}$, the results in Table 2 show a large scatter with a little positive correlation with the experiments.

$$\varsigma_1 = \sqrt{\frac{2G_{If}(t)E_s\rho_s}{d\lambda^2\, w(t)/w(t_0)(a_c+a_{cc})^2}\left[\frac{9}{26}(0.8d+a_{cc})^2+0.72d^2\right]\frac{1}{v_u^2}+ \frac{21.034C_f\,a_{cc}[0.0255f_c(t)+1.024]^2[f_c(t)]^{0.7}}{v_u^2 d\lambda^2\, w(t)/w(t_0)(a_c+a_{cc})^2}\left[0.9d+\frac{3a_{cc}}{2}+\frac{a_{cc}^2}{0.8d}\right]} \tag{59}$$

Nevertheless, development of the diagonal deformations, which were presented in Part I of this paper, is an alternative for the crack width ratio, as the LVDT's used to measure the diagonal deformations cover the critical shear cracks. As shown in Part I of this paper, the development of the diagonal deformation at one side (right or left) is larger than at the other side. In the row regarding the $DD(t)/DD(t_0)$ in Table 2, the maximum diagonal deformation is given for each beam. The shear safety margin ς_2, which is calculated according to the diagonal deformation ratio of each specimen, is given in the last row of Table 2:

$$\varsigma_2 = \sqrt{\frac{2G_{If}(t)E_s\rho_s}{d\lambda^2\, DD(t)/DD(t_0)(a_c+a_{cc})^2}\left[\frac{9}{26}(0.8d+a_{cc})^2+0.72d^2\right]\frac{1}{v_u^2}+ \frac{21.034C_f\,a_{cc}[0.0255f_c(t)+1.024]^2[f_c(t)]^{0.7}}{v_u^2 d\lambda^2\, DD(t)/DD(t_0)(a_c+a_{cc})^2}\left[0.9d+\frac{3a_{cc}}{2}+\frac{a_{cc}^2}{0.8d}\right]} \tag{60}$$

The results show consistent trends with respect to the beams which have failed (S4B6 and S7B6) and those which have persisted:

Table 2. Comparison of the experimental results with shear safety parameter

Specimen	S2B4	S2B5	S2B6	S3B5	S3B6	S4B4	S4B5	**S4B6***	S5B4	S5B6	S6B4	S6B6	S7B5	**S7B6****
Load intensity factor, λ	0.88	0.88	0.88	0.97	0.97	0.95	0.95	0.98	0.92	0.86	0.92	0.92	0.93	0.91
Age at the beginning, t_0 [days]	72	72	72	87	87	71	71	71	512	696	113	113	219	219
Age at the end, t [days]	156	156	156	1431	214	345	345	71	1296	1296	>1226	1226	>1160	221
$f_{cm}(t_0)$ [MPa]	31.1	31.1	31.1	40.8	40.8	40.2	40.2	40.2	43.9	44.3	71.4	71.4	74.9	74.9
$f_{cm}(t)$ / $f_{cm}(t_0)$	1.05	1.05	1.05	1.11	1.05	1.09	1.09	1.00	1.02	1.01	1.02	1.02	1.00	1.00
$V_{u.exp}$ / $V_{u.calc}(t)$	1.05	1.04	1.07	1.05	0.96	1.13	1.15	0.98	1.13	0.95	-	1.19	-	1.00
Critical crack number	11	1	1,3	13,14	1,2	12	10	-	2,5	12	13,14	14	15	-
$\Delta(t)/\Delta(t_0)$	1.28	1.22	1.24	1.55	1.24	1.56	1.38	1.38	1.35	1.45	1.40	1.46	1.29	1.08
$[w(t)/w(t_0)]_{mean}$	1.08	1.05	1.06	1.30	1.06	1.32	1.15	1.15	1.14	1.10	1.13	1.16	1.13	1.01
$[w(t)/w(t_0)]_{max}$	-	-	-	-	-	-	-	-	0.53	0.52	0.18	0.31	0.5	-
$DD(t)/DD(t_0)$	1.11	1.31	1.07	1.14	1.28	1.21	1.23	1.83	1.19	1.42	1.00	1.07	1.16	1.47
$G_f(t_0)$	0.136	0.136	0.136	0.142	0.142	0.142	0.142	0.142	0.144	0.144	0.157	0.157	0.159	0.159
G_{fII}	0.107	0.107	0.107	0.127	0.127	0.126	0.126	0.126	0.134	0.135	0.204	0.204	0.214	0.214
$G_f(t)$ / $G_f(t_0)$	1.01	1.01	1.01	1.02	1.01	1.02	1.02	1.00	1.00	1.00	1.00	1.00	1.00	1.00
$v_u = V/bd$ [MPa] Eq. 52	1.08	1.08	1.08	1.18	1.18	1.17	1.17	1.17	1.21	1.22	1.26	1.26	1.28	1.28
ς_1 (using the mean crack width)	1.11	1.12	1.12	0.94	1.02	0.95	1.01	0.95	1.03	1.11	1.03	1.02	1.01	1.10
ς_2 (using diagonal deformation)	1.10	1.01	1.11	1.00	0.93†	1.00	0.99	**0.75***	1.00	0.98	1.09	1.06	1.00	**0.91****

* Beam S4B6 failed after 2.5 hours under sustained loading
** Beam S7B6 failed after 44 hours under sustained loading
† Beam S3B6 failed after one cycle reloading and unloading

The lowest values of ς_2 are 0.75 and 0.91, which refer to the specimens S4B6 and S7B6, respectively. The former failed after 2.5 hours and the latter failed after 44 hours under sustained loading. Specimen S3B6 with a shear safety margin ς_2 of 0.93, persisted the sustained loads for 127 days, but failed after 1 cycle of unloading and reloading with a shear resistance equal to $V_{u,\text{calc }5\%}$.

Specimen S5B6 with a shear safety margin ς_2 of 0.98, persisted the sustained loading for 600 days. At the end of the program, when the beam was loaded to failure, a shear resistance equal to $V_{u,\text{calc }5\%}$ was obtained. The rest of the beams with shear safety margin above 1.0 persisted under sustained loading.

The values of the shear safety margin ς_2, which are calculated according to Eq. 60 are rather conservative. That is due to the fact that the ratio of $DD(t)/DD(t_0)$ refers to the opening of two or more shear cracks in time and this causes an underestimation of the shear resistance under sustained loading $v_{cr}(t)$.

For a more convenient interpretation of the results, the values of the shear safety margin ς_2 are plotted versus the DD(t) / DD(t0) ratio in Fig 14. The data can be associated with a linear trend-line. This graph represents the shear safety margin, with respect to the development of the diagonal deformation in time in the reinforced concrete beam. The solid line in Fig. 14 represents the mean prediction, whereas the dashed lines represent the 5% confidence limits. When the diagonal deformation increases with more than 25% of the initial value $DD(t_0)$, the shear safety margin is generally lower than 1.0.

In Fig 13a, the shear safety margin ς_2 is plotted versus the load intensity factor. According to this graph, the shear safety margin reduces generally when the load intensity increases. The shear safety margin can be lower than 1.0 when the load intensity is larger than 0.92.

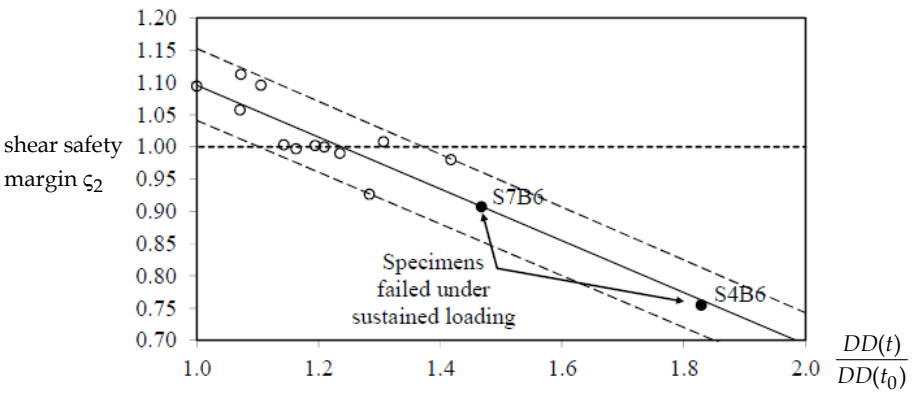

Figure 12. Shear safety margin versus the DD(t) / DD(t0) ratio

However, a load intensity equal to 0.92 is beyond the characteristic value of the short-term shear resistance.

According to Table 2 in Part I of this paper (Sarkhosh, 2014) the ratio of the lower confidence limit of shear resistance to the mean value in Series 7, which has the largest coefficient of variation, equals $LCL_{5\%}/V_{u,\text{mean}} = 0.9$. The shadowed area in Fig. 15b represents the load intensities larger than the characteristic value of the shear resistance. As a conclusion, a shear safety margin greater than 1.0 is expected for the specimens loaded up to the characteristic value of the short-term shear resistance.

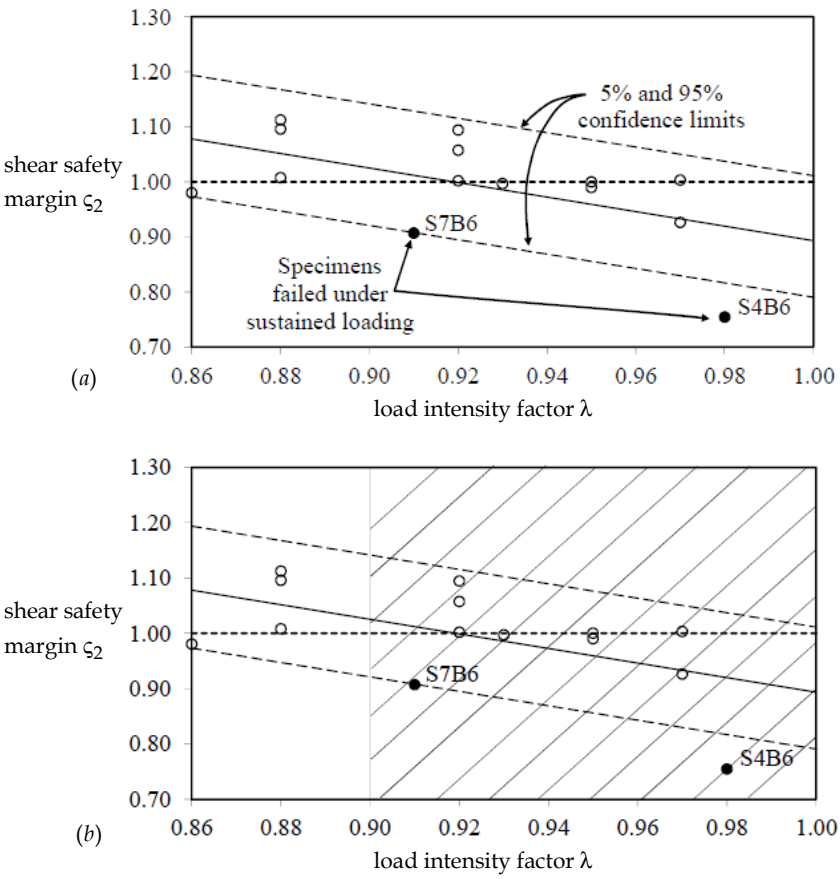

Figure 13. Shear safety margin versus the load intensity λ ; the shadowed area in figure (b) represents the scatter of the shear resistance (5% fractile) according to the short-term monotonic tests

8 Conclusions

- With respect to the time-dependent parameters in Eq. (54), a parametric study was conducted to investigate the effect of each variable on the shear safety margin ς. The most significant decrease of ς is related to the load intensity and crack opening displacement in time. The increase of the material properties of concrete such as $G_f(t)$ and $f_c(t)$ shows a positive effect on the shear safety margin: yet the influence of an increase of the compressive strength is likely to be insignificant.
- With the shear model developed in this study, based on a bilinear shear crack, it is possible to mobilize the contribution of aggregate interlock in a consistent way. The aggregate interlock contribution develops in the lower part of the inclined shear crack, due to crack rotation around the crack tip in the upper part. In this way the crack faces are subject to inverse shear displacement of the crack faces and generate the interlock stresses contributing to the shear resistance.
- The bilinear shape of the shear crack represents a significant improvement in modelling against former models based on a linear crack shape in predicting the shear resistance in a consistent way. Further improvements in this development have meanwhile been developed at TU Delft (Yang, 2014)
- Aggregate interlock is as well an important element for the explanation why sustained loading does not have to be regarded in shear. Aggregate interlock shows a hardening behavior. Crack sliding leads to an increased aggregate interlock resistance, which compensates for other time dependent effects.
- This study has demonstrated that although reinforced concrete beams under sustained loading with high load intensity deform due to creep and some cracks open in time, no reduction of the shear resistance is reported at the end of long-term loading. Accordingly, no reduction factor is required for shear resistance of reinforced concrete beams without stirrups under sustained loading.

References

ACI Committee 318, (2008), Building Code Requirements for Structural Concrete 318-08, and Commentary (318R-08), American Concrete Institute, Farmington Hills

Bažant, Z. P., and Yu, Q. (2004), "Designing against Size Effect on Shear Strength of Reinforced Concrete Beams without Stirrups - Part I: Formulation, Part II: Verification and Calibration," *ASCE Journal of Structural Engineering*, Vol. 131, No. 12, pp. 1877-1897

Bhal, N. S. (1968), *On the Influence of Beam Depth on Shear Capacity of Single-Span RC Beams with and without Shear Reinforcement*, PhD dissertation, Universität Stuttgart, Stuttgart, Germany, pp. 1-124

BS 8110, (1997), Code of Practice for Design and Construction, 2nd Edition, British Standards Institution, London, UK, 168 pp.

Canadian Standards Association (CSA), (2004), Design of concrete structures A23.3-04, Mississauga, Ontario. 232 pp.

Clark, L.A. and Spiers, D.M. (1978), Tension stiffening in reinforced concrete beams and slabs under short-term load, Technical Report No. 42.521, Cement and Concrete Association, Wexham Springs

EN 1992-1-1-2005, Eurocode 2; Design of Concrete Structures, Part 1-1: General Rules and Rules for Buildings, Committee of European Normalisation (CEN), (1992–2005a), Brussels

FIB, Model Code 2010, fib Bulletin No. 65, Final draft, Volume 1, March 2012

Frénaij, J.W. (1989), *Time-dependent shear transfer in cracked reinforced concrete*, Doctoral Thesis, Delft University of Technology, Delft, the Netherlands, 183 pp.

Frénay, J.W. (1990), "Theory and experiments on the behaviour of cracks in concrete subjected to sustained shear loading," *HERON*, Vol. 35, No. 1, 58 pp.

Frénay, J.W., Reinhardt, H. W. and Walraven, J. C. (1991), "Time-dependent shear transfer in cracked concrete: Part I and II," *ASCE J. Struct. Eng*. Vol. 117, No. 10, pp. 2900-2935.

Gastebled, O.J, and May, I.M. (2001), "Fracture Mechanics Model Applied to Shear Failure of Reinforced Concrete Beams without Stirrups," *ACI Structural Journal*, Vol. 98, Issue 2, pp. 184-190

Gilbert, R.I. and Warner, R.F. (1978), "Tension stiffening in reinforced concrete slabs," *ASCE Journal of the Structural Division*, Vol. 104, ST. 12, pp. 1885- 1900

Hsu, T.T.C. and Zhang, L.X. (1996), "Tension stiffening in reinforced concrete membrane elements," *ACI Structural Journal*, Vol. 93, No.1, pp. 108-115

Kotsovos, M.D. and Bobrowski, J. (1993) "Design model for structural concrete based on the concept of the compression force path," *ACI Structural Journal*, Vol. 90, No. 1, pp. 12-20

Lárusson, L., Fischer, G. and Jönsson, J. (2012), "Mechanical Interaction between Concrete and Structural Reinforcement in the Tension Stiffening Process", In: High Performance

Fiber Reinforced Cement Composites, Eds. G.J. Parra-Montesinos, H.W. Reinhardt, and A.E. Naaman: HPFRCC, Vol. 6, pp. 247-254

Marti, P., Alvarez, M., Kaufmann, W. and Sigrist, V. (1998), "Tension chord model for structural concrete," *IABSE Structural Engineering International*, Vol. 8 No. 4, pp. 287-298

Reineck, K.H. (1991), "Ultimate Shear Force of Structural Concrete Members Without Transverse Reinforcement Derived From a Mechanical Model," *ACI Structural Journal*, Vol. 88, Issue 5, pp. 592-602

Reineck, K.H., Bentz, E.C., Fitik, B., Kuchma, D.A., and Bayrak, O., (2013), "ACI-DAfStb Database of Shear Tests on Slender Reinforced Concrete Beams without Stirrups," *ACI Struct J.*, Vol. 110, No. 5, pp. 867-876

Sarkhosh, R. (2014), *Shear Resistance of Reinforced Concrete Beams without Shear Reinforcement under Sustained Loading*, PhD Dissertation, Delft University of technology, Delft, Netherlands, pp. 259

Sarkhosh, R., Walraven, J. and den Uijl, J., (201X), "Shear-Critical Reinforced Concrete Beams under Sustained Loading - Part I: Experiments", *HERON* Vol. 60 (2015) No. 3

Taylor, H.P.J. (1972), "Shear Strength of Large Beams," *ASCE Journal* of the Structural Division, Vol. 98 No. 11, pp. 2473-2490

Walraven, J.C. (1978), The influence of depth on the shear strength of light-weight concrete beams without shear reinforcement, Stevin report 5-78-4, Delft Univ. of Technology, 36 pp.

Walraven, J. C. (1980), *Aggregate interlock: a theoretical and experimental analysis*, Doctoral thesis, Delft University of Technology, 197 pp.

Wu, H.Q. and Gilbert, R. (2008), An Experimental Study of Tension Stiffening in Reinforced Concrete Tension Members under Short-Term and Long-Term Service Loads, UNICIV Report No. R-449, the University of New South Wales, Sydney, Australia

Wu, M. H. Q. (2010), *Tension stiffening in reinforced concrete: instantaneous and time-dependent behaviour*, Doctoral Thesis, University of South Wales, Sydney, Australia

Xu, S., Zhang, X. and Reinhardt, H.W., 2012, "Shear Capacity Prediction of Reinforced Concrete Beams without Stirrups Using Fracture Mechanics Approach," *ACI Structural Journal*, Vol. 109, Issue 5, pp. 705-714

Yang, Y., (2014), *Shear Behaviour of Reinforced Concrete Members without Shear Reinforcement*, PhD Thesis Delft University of Technology, April 2015